

# A three-dimensional carbon-coated LiFePO<sub>4</sub> electrode for high-power applications

Catia Arbizzani · Sabina Beninati ·  
Marina Mastragostino

Received: 11 March 2009 / Accepted: 9 June 2009 / Published online: 20 June 2009  
© Springer Science+Business Media B.V. 2009

**Abstract** The fabrication process of a new, three-dimensional carbon-coated LiFePO<sub>4</sub> electrode by sol–gel synthesis in situ on interconnected conducting fibers of carbon paper is described. This three-dimensional structure ensures overall electrode conductivity, facilitates lithium diffusion in and out of LiFePO<sub>4</sub> particles and, hence, enables good cycling stability at 1C-rate and maximum pulse-power values that exceed those of planar LiFePO<sub>4</sub> electrodes at high electrode loading.

**Keywords** Lithium iron phosphate · Lithium-ion batteries · Three-dimensional electrode · Maximum specific pulse-power

## 1 Introduction

Lithium ion is the battery of choice for sustainable transportation by strong-HEVs in which a synergic combination of the internal combustion engine and batteries provides high fuel utilization with benefits for fuel economy and greenhouse-gas emission. The requirements for power-assist HEVs are pulse (discharge/regenerative) power of 620 W kg<sup>-1</sup> for 10 s over more than 3 × 10<sup>5</sup> shallow cycles and 7.5 Wh kg<sup>-1</sup> total available energy [1]. Much R&D effort has been focused on new generation Li-ion batteries for application in strong-HEVs. While batteries of different chemistry already meet the power requisite, some concerns still remain about their safety mainly because of

the tolerance to abusive conditions that may trigger dangerous, thermal runaway reactions [2]. LiFePO<sub>4</sub> is a non-toxic lithium intercalation compound with a theoretical capacity of 170 Ah kg<sup>-1</sup> featuring low cost and thermal stability and is one of the most preferred cathode materials. It is, indeed, more stable than transition metal oxides against oxygen release, which is responsible for dangerous oxidation reactions of the organic electrolytes [3]. The high-power Li-ion batteries based on LiFePO<sub>4</sub> already on the market feature nominal energy of 80–100 Wh kg<sup>-1</sup>.

Given that LiFePO<sub>4</sub> displays poor electronic conductivity and a low lithium ion diffusion coefficient, even nano-particles doped by polyvalent cations and coated by carbon have been synthesized by different routes, including the presence of nanocarbons (CNF and MWCNT). Nano-structured LiFePO<sub>4</sub> planar electrodes have thus been prepared by adding binder and conducting carbon [4–7]. We report a different approach based on sol–gel synthesis of carbon-coated LiFePO<sub>4</sub> on the interconnected conducting fibers of the carbon paper used as support-current collector and demonstrate that this in situ synthesis provides a three-dimensional electrode enabling discharge pulses of higher maximum specific-power and energy efficiency than conventional planar LiFePO<sub>4</sub> electrodes.

## 2 Experimental

The chemicals for sol–gel synthesis of carbon-coated LiFePO<sub>4</sub> were home-made Fe(III)-citrate, C<sub>6</sub>H<sub>5</sub>FeO<sub>7</sub>, prepared according to [8], and commercial H<sub>3</sub>PO<sub>4</sub> and Li<sub>3</sub>PO<sub>4</sub> from Sigma-Aldrich. The C<sub>6</sub>H<sub>5</sub>FeO<sub>7</sub> was prepared by dissolving 5 g ca. of Fe(III) chloride (Sigma Aldrich) in deionized water and adding the stoichiometric amount of NaOH to precipitate Fe(OH)<sub>3</sub>, which was filtrated and water

C. Arbizzani · S. Beninati · M. Mastragostino (✉)  
Department of Metal Science, Electrochemistry and Chemical  
Techniques, University of Bologna,  
Via San Donato 15, 40127 Bologna, Italy  
e-mail: marina.mastragostino@unibo.it

washed. An aqueous solution of citric acid (Fluka) was then added to  $\text{Fe}(\text{OH})_3$  to form a ferric-organic solution that was heated at  $90^\circ\text{C}$  for 2 h under stirring. After solution cooling at room temperature, acetone was added to precipitate the  $\text{Fe}(\text{III})$ -citrate, which was separated and acetone washed. The purity grade of the home-made  $\text{C}_6\text{H}_5\text{FeO}_7$  was 95% as estimated by spectrophotometric measurements as follows: a few mg of  $\text{Fe}(\text{III})$ -citrate were dissolved in 0.2 M  $\text{HNO}_3$  and mixed with a solution of potassium thiocyanate (Sigma Aldrich) to form an intensely colored complex with maximum absorbance at 480 nm; the molar absorption coefficient at this wavelength, evaluated by a standard solution of  $\text{Fe}(\text{III})$ -nitrate in 0.5 M  $\text{HNO}_3$  from Merck, was  $\varepsilon = 9.73 \times 10^3 \text{ L mol}^{-1} \text{ cm}^{-1}$ . The carbon paper (CP) was from Spectracorp (Spectracarb 2050, density  $0.42 \text{ g/cm}^3$ , thickness  $200 \mu\text{m}$ ), and disks of geometric area of  $0.60 \text{ cm}^2$  were cut, washed with acetone, and dried under vacuum for 2 h before use.

The fabrication of three dimensional electrodes by the sol-gel synthesis of carbon-coated lithium iron phosphate on interconnected conducting fibers of CP was performed as follows: 2 g of  $\text{Fe}(\text{III})$ -citrate were dissolved along with  $\text{H}_3\text{PO}_4$  and  $\text{Li}_3\text{PO}_4$  in stoichiometric molar ratio in 50 mL of water and the solution was heated at  $60^\circ\text{C}$  under stirring until its volume was reduced to 30% ca. of the initial value. The concentrated solution was then used to imbibe the CP disks under vacuum to ensure that all the inner fibers were covered. The impregnated disks were kept for 2 days at  $60^\circ\text{C}$  for xerogel formation on the carbon fibers, heated in tubular furnace up to  $700^\circ\text{C}$  (at  $20^\circ\text{C min}^{-1}$ ) and kept there for 1 h under 5%  $\text{H}_2$ -Ar flux ( $300 \text{ mL min}^{-1}$ ). Thereafter, three-dimensional, carbon-coated lithium iron phosphate (3D  $\text{LiFePO}_4/\text{C-CP}$ ) electrodes,  $200 \mu\text{m}$  thick and with active material loading per geometric area of ca.  $10 \text{ mg cm}^{-2}$  but without any binder or carbon additive, were ready for use. Similar heating tests performed on bare CP disks demonstrated that no mass loss of the three-dimensional current collector occurred.

Separately, a portion of the concentrated sol-gel solution was thermally treated at the same conditions to prepare  $\text{LiFePO}_4/\text{C}$  powder for X-ray diffraction (XRD) and thermogravimetric analysis (TGA). The XRD analyses were performed by a Philips PW1710 diffractometer, a  $\text{Cu K}_\alpha$  ( $\lambda = 1.5406 \text{ \AA}$ ) radiation source and Ni filter with continuous acquisition in  $5\text{--}80^\circ 2\theta$  range,  $0.025^\circ 2\theta \text{ s}^{-1}$  scan rate and the TGA was carried out by Mettler Toledo TGA/SDTA A851 from room temperature (RT) to  $700^\circ\text{C}$  (heating rate  $5^\circ\text{C min}^{-1}$ ) in  $\text{O}_2$  flux. The scanning electron micrograph (SEM) images were acquired by a Zeiss EVO 50 apparatus.

Electrochemical characterization of the three-dimensional  $\text{LiFePO}_4/\text{C-CP}$  electrodes was carried out in T-type cell with Li as reference and Li in excess as counter

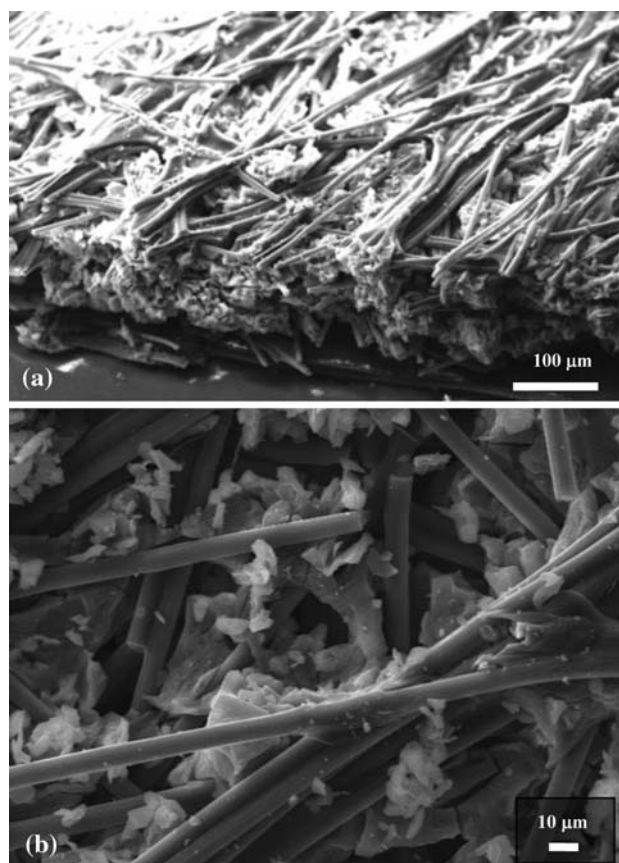
electrode; a dried and degassed glass separator (Whatman GF/D  $400 \mu\text{m}$  thick) was used after soaking in the same electrolyte of the electrochemical cell ethylene carbonate (EC):dimethylcarbonate (DMC) 2:1-1 M  $\text{LiPF}_6$  (Merck LP31). Cell assembling and sealing were performed in argon atmosphere MBraun Labmaster 130 dry box ( $\text{H}_2\text{O}$  and  $\text{O}_2 < 1 \text{ ppm}$ ) and the electrochemical tests were performed by Perkin-Elmer VMP multichannel potentiostat.

### 3 Results and discussion

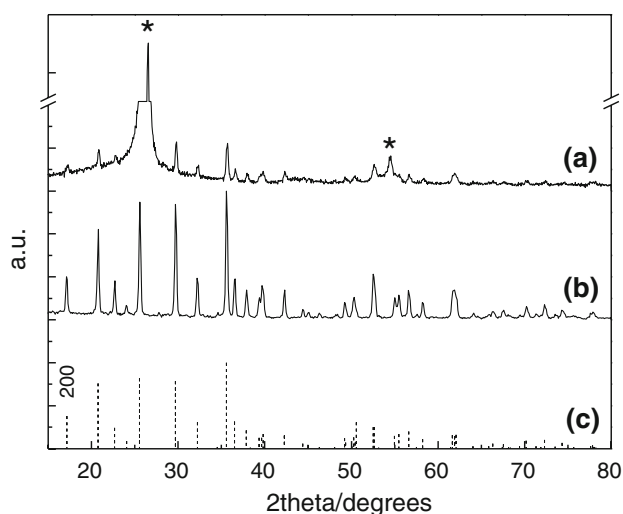
#### 3.1 SEM, XRD, and TGA characterization

Figure 1 shows SEM images of the 3D  $\text{LiFePO}_4/\text{C-CP}$  electrode. Image (a), which was acquired with the sample tilted to show the morphology of the cross-section, demonstrates that the synthesized particles are evenly distributed throughout the network of carbon fibers; image (b) shows that particle sizes are comparable to the diameter of the carbon fibers (ca.  $10 \mu\text{m}$ ).

Figure 2 shows the XRD patterns of the 3D  $\text{LiFePO}_4/\text{C-CP}$  electrode and of the  $\text{LiFePO}_4/\text{C}$  powder compared to



**Fig. 1** SEM images of 3D  $\text{LiFePO}_4/\text{C-CP}$  electrode at two magnifications



**Fig. 2** (a) XRD pattern of 3D LiFePO<sub>4</sub>/C-CP electrode, (b) XRD pattern of LiFePO<sub>4</sub>/C powder and (c) reference powder diffraction file of LiFePO<sub>4</sub> (81–1,173) from ICDD database. A star indicates the CP peaks

the reference powder diffraction file of LiFePO<sub>4</sub> from ICDD database. All the peaks, excluding the marked CP signals, are related to LiFePO<sub>4</sub>, thereby demonstrating the efficacy of the citrate ion in the reduction of Fe(III) to Fe(II). Sampled from different syntheses, the crystallite sizes of the LiFePO<sub>4</sub>, as evaluated by Scherrer's equation from the 200 peak of the powder XRD spectra to avoid CP signal interference, were in the range of 30–37 nm.

The carbon content in carbon-coated lithium iron phosphate was evaluated via TGA analysis by heating a LiFePO<sub>4</sub>/C powder sample in O<sub>2</sub> flux from RT up to 700 °C. The oxygen burns off the carbon and causes the complete oxidation of LiFePO<sub>4</sub> to Li<sub>3</sub>Fe<sub>2</sub>(PO<sub>4</sub>)<sub>3</sub> and Fe<sub>2</sub>O<sub>3</sub>, as demonstrated in [9]. We then estimated that the carbon content in the LiFePO<sub>4</sub>/C samples was ca. 8.2 wt% by considering a theoretical 5.1% mass increase due to the LiFePO<sub>4</sub> oxidation and a 3.1% experimental mass decrease with respect to the initial mass. Figure 3 shows the TGA of a carbon-coated LiFePO<sub>4</sub> powder sample.

### 3.2 Electrochemical tests

Given that the CP matrix of these novel 3D electrodes should facilitate electronic transport and lithium diffusivity, cells with 3D LiFePO<sub>4</sub>/C-CP electrodes of high active material loading, ca. 10 mg cm<sup>-2</sup> of geometric area, were tested at 30 °C by repeated galvanostatic charge–discharge cycles at 1C, which is the C-rate suggested by DOE to calculate available energy of batteries for HEV application (FreedomCAR Battery Test Manual For Power-Assist Hybrid Electric Vehicles, <http://www.uscar.org>). Figure 4 displays the delivered capacity over 400 deep cycles

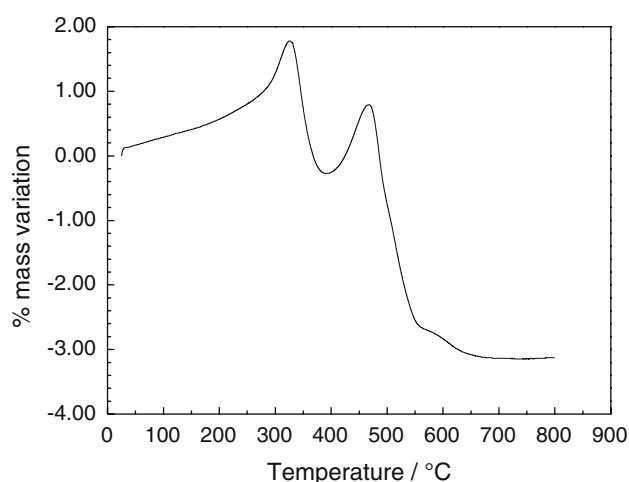


**Fig. 3** TGA trace of a carbon-coated LiFePO<sub>4</sub> powder sample

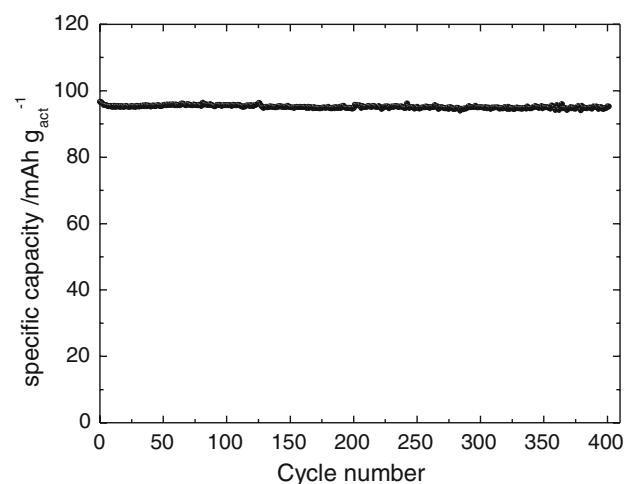


**Fig. 4** Cycling stability of 3D LiFePO<sub>4</sub>/C-CP electrode ( $m_{\text{act}} = 10.1 \text{ mg cm}^{-2}$ ) over 400 galvanostatic cycles at 1C and 30 °C

between 4.3 and 2.2 V versus Li. The delivered capacity remains constant over all the cycles at ca. 100 m Ah g<sup>-1</sup> of LiFePO<sub>4</sub>, thereby demonstrating the high cycling-stability of these 3D LiFePO<sub>4</sub>/C electrodes. The difference in the charge–discharge voltage plateaus at this C-rate was ca. 120 mV, a sufficiently low value which demonstrates that the morphology of these 3D electrodes with distributed LiFePO<sub>4</sub>/C particles on interconnected carbon conducting fibers enables easy electronic charge transport and facilitates lithium diffusion into lithium iron phosphate particles. The 3D electrodes, charged at 1C, were also discharged at higher C-rates than 1C and Fig. 5 shows the voltage profiles of discharge curves from 1C to 5C of the same electrode in Fig. 4, recorded after 400 cycles at C1 and 1 month of shelf-life. The delivered charge at 5C discharge rate is 85% of that delivered at 1C, thus demonstrating the high-rate

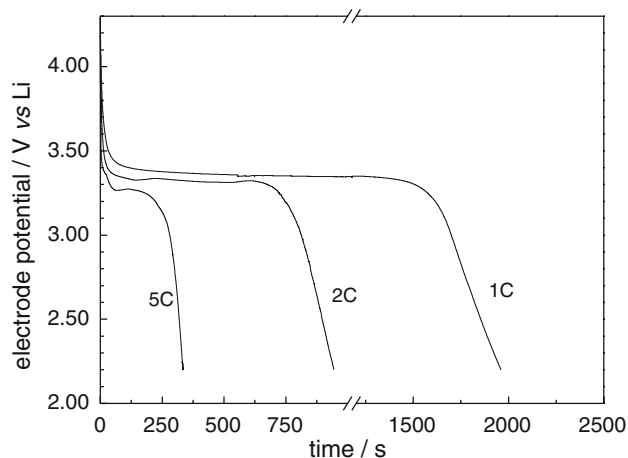


**Fig. 5** Discharge voltage profiles at 30 °C and at different C-rates of the 3D LiFePO<sub>4</sub>/C electrode in Fig. 4 charged at 1C

capability of these 3D electrodes. Note too that the carbon content is 8.2 wt%, a value lower than that generally present in conventional composite electrodes (15 wt%). CP is thus a good current collector-substrate even for cathode materials which are intrinsically poor electronic conductors like LiFePO<sub>4</sub>.

In order to evaluate the maximum pulse power of these 3D LiFePO<sub>4</sub>/C-CP electrodes with active material loading of ca. 10 mg cm<sup>-2</sup>, 10 sequences of 10 s pulses (10 s discharge, 300 s rest and 10 s charge) at high C-rates from 5C to 35C were performed. The pulse tests were carried out after discharging the cell at C/10 down to 50% DOD; the power values at each C-rate were evaluated at the last pulse sequence as the discharge energy divided by the 10 s pulse time. These power values, which are referred to the active material mass ( $P_{act}$ ) or to the total electrode mass, including CP ( $P_{el}$ ), were then plotted versus C-rate, as was the end-voltage of the discharge and charge pulses. The maximum pulse power ( $P_{max}$ ) was evaluated by interpolation of the plots from the discharge at the maximum C-rate which provides charge/discharge pulses within a voltage window of 2.20–4.00 V. Maximum voltage,  $V_{max}$ , was set at 4.00 V to compare the resulting data with those of planar electrodes reported in [10], and minimum voltage,  $V_{min}$ , was set at  $0.55 \times V_{max} = 2.20$  V, according to US Advanced Battery Consortium and DOE standards for HEV battery applications (FreedomCAR Battery Test Manual For Power-Assist Hybrid Electric Vehicles, <http://www.uscar.org>). The pulse energy efficiency at the maximum power ( $\eta_p$ ) was also calculated as the ratio of the experimentally delivered energy to that which would be provided if all the charge were delivered at the voltage plateau of 3.4 V without any irreversible potential loss during the 10 s discharge pulse.

Figure 6 reports these plots and shows that the maximum allowed C-rate and, consequently, the maximum

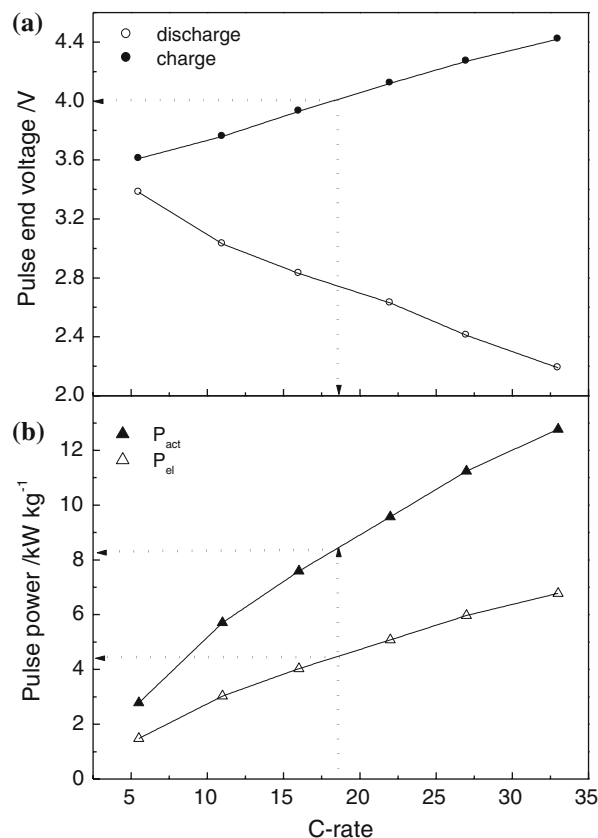


**Fig. 6** **a** Cell end-voltage values of discharge and charge pulses versus C-rate. **b** Specific power values referred to active material mass or total electrode mass versus C-rate of 3D LiFePO<sub>4</sub>/C-CP electrode ( $m_{act} = 10.7$  mg cm<sup>-2</sup>)

power are established by reaching the upper limit voltage (4.00 V). Accordingly, Table 1 summarizes the values of maximum pulse specific power,  $P_{max,act}$  and  $P_{max,el}$  at the maximum C-rate, of specific current at the maximum C-rate ( $J_{max}$ ) and of pulse efficiency at the maximum pulse power ( $\eta_p$ ) for these electrodes with active material loading of ca. 10 mg cm<sup>-2</sup> and total electrode mass, including CP of ca. 20 mg cm<sup>-2</sup>. These 3D LiFePO<sub>4</sub>/C-CP electrodes, 200  $\mu$ m thick, show  $P_{max,act}$  values of 8.4 kW kg<sup>-1</sup> and  $P_{max,el}$  of 4.5 kW kg<sup>-1</sup>. However, the  $P_{max,el}$  is still a high value compared to the best performing planar LiFePO<sub>4</sub> electrodes with comparable loading of active material and meets the USABC power goal of 2 kW kg<sup>-1</sup> of total cathode mass. Furthermore, if  $V_{max}$  were set at 4.20 V (a feasible value) and  $V_{min}$  at 2.31 V, the maximum allowed C-rate would be 23C and, hence, the maximum specific power values of these 3D LiFePO<sub>4</sub>/C-CP would be 20% higher. The 82% energy efficiency of these 3D electrodes is also higher than that of planar electrodes (60–70%) [10]. These results are consistent with expectations, i.e., that the CP matrix of these novel 3D electrodes facilitates lithium mass transport in/out of the LiFePO<sub>4</sub> because of the high

**Table 1** Active material loading, electrode mass,  $P_{\max,act}$ ,  $P_{\max,el}$ , maximum C-rate,  $J_{\max}$ , and  $\eta_P$  of 3D LiFePO<sub>4</sub>/C-CP electrode

Active material loading (mg cm <sup>-2</sup> )	Electrode mass (mg cm <sup>-2</sup> )	$P_{\max,act}$ (kW kg <sup>-1</sup> )	$P_{\max,el}$ (kW kg <sup>-1</sup> )	Maximum C-rate	$J_{\max}$ (A g <sub>act</sub> <sup>-1</sup> )	$\eta_P$ (%)
10.7	20.2	8.4	4.5	18.5	3.2	82

surface area in contact with the electrolyte, which makes the LiFePO<sub>4</sub> solid-phase of these electrodes thinner than that of conventional planar electrodes, particularly at high loading of active material.

These 3D LiFePO<sub>4</sub>/C-CP electrodes also display a maximum pulse power per geometric area that compares well to that of newly developed LiFePO<sub>4</sub> electrodes with conventional composite (LiFePO<sub>4</sub>/C, carbon additive and PVdF-binder) loaded into a three-dimensional porous Ni–Cr alloy current collector. In fact, when loaded with ca. 15 mg cm<sup>-2</sup> of active material, the latter displayed under 2 s pulse tests a maximum pulse power of 0.12 W cm<sup>-2</sup>, but the mass of the NiCr support is 45 mg cm<sup>-2</sup> instead of the 10 mg cm<sup>-2</sup> of CP. Therefore, the specific power value of the 3D LiFePO<sub>4</sub>/C-CP electrodes is better than that of the LiFePO<sub>4</sub>/C-NiCr electrodes [11].

#### 4 Conclusions

Direct sol–gel synthesis of carbon-coated LiFePO<sub>4</sub> on interconnected conducting fibers of CP yielded three-dimensional electrodes featuring high cycling stability over 400 deep charge–discharge cycles at 1C-rate and maximum 10 s-pulse power of 4.5 kW kg<sup>-1</sup> (including CP mass), which is higher than that of planar LiFePO<sub>4</sub> electrodes at the high active material loading of ca. 10 mg cm<sup>-2</sup>. High pulse-power performance at electrode loading of practical use in batteries clearly demonstrates that the unique morphology of interconnected carbon micrometric fibers

evenly covered by lithium iron phosphate greatly improves the electronic and ionic mass transport in LiFePO<sub>4</sub> and makes it possible to develop high-power batteries for HEV application based on this ion-insertion material.

**Acknowledgments** The assistance of Ms. Stefania Stabile is acknowledged and appreciated. Research funded by MIUR under the Italian Project PRIN 2005.

#### References

1. Stewart SG, Srinivasan V, Newman J (2008) J Electrochem Soc 155:A664
2. Jiang J, Dahn JR (2004) Electrochem Commun 6:39
3. Wohlfahrt-Mehrens M (2007) Routes to improve lithium iron phosphate for battery applications, Chap. 17, Lithium Mobile Power 2007, October 29–30 2007, San Diego, CA, p 337
4. Chung SY, Blocking JT, Chiang YM (2002) Nat Mater 1:123
5. Ravet N, Chouinard Y, Magnan JF, Besner S, Gautier M, Armand M (2001) J Power Sources 97:503
6. Bhunaneswari MS, Bramnik NN, Ensling D, Ehrenberg H, Jaegerman W (2008) J Power Sources 180:553
7. Li X, Kang F, Bai X, Shen W (2007) Electrochem Commun 9:663
8. Chan K, Town W (2007) Pharmaceutical-grade ferric organic compounds, uses thereof and methods of making same, World Intellectual Property Organization Patent No WO 2007/02/2435
9. Belharouack I, Johnson C, Amine K (2005) Electrochem Comm 7:983
10. Thorat IV, Mathur V, Harb JN, Wheeler DR (2006) J Power Sources 162:678
11. Yao M, Okuno K, Iwaki T, Kato M, Tanese S, Emura K, Sakai T (2007) J Power Sources 173:545